

The lifetime of grand design

M.R. Merrifield,^{1*} R.J. Rand² and S.E. Meidt²

¹*School of Physics & Astronomy, University of Nottingham, University Park, Nottingham, NG7 2RD*

²*Department of Physics and Astronomy, University of New Mexico, 800 Yale Boulevard Northeast, Albuquerque, NM 87131, USA*

Accepted 2005 November 1. Received 2005 October 21; in original form 2005 September 17

ABSTRACT

The lifetime of the structure in grand design spiral galaxies is observationally ill-determined, but is essentially set by how accurately the pattern’s rotation can be characterized by a single angular pattern speed. This paper derives a generalized version of the Tremaine–Weinberg method for observationally determining pattern speeds, in which the pattern speed is allowed to vary arbitrarily with radius. The departures of the derived pattern speed from a constant then provides a simple metric of the lifetime of the spiral structure. Application of this method to CO observations of NGC 1068 reveal that the pattern speed of the spiral structure in this galaxy varies rapidly with radius, and that the lifetime of the spiral structure is correspondingly very short. If this result turns out to be common in grand-design spiral galaxies, then these features will have to be viewed as highly transient phenomena.

Key words:

galaxies: spiral – galaxies: kinematics and dynamics – galaxies: structure – galaxies: individual: NGC 1068

1 INTRODUCTION

Spiral arms are some of the most strikingly beautiful features of galaxies, yet even now we lack a full understanding of their origins. It is well known that these features cannot simply be interpreted as long-lived aesthetically-organized “material spirals” of particularly bright stars – as stressed by Oort (1962), the strong differential rotation in disk galaxies would rapidly wind up and destroy any such arrangement. It was this “winding dilemma” that motivated Lin & Shu (1966) to build on the earlier intuition of Lindblad (1951) and develop a theory by which spirals could persist as long-lived density waves, thereby apparently solving the problem. However, ever since this theory was first espoused, questions have remained. For example, Toomre (1969) argued that such spiral density waves would tend to dissipate on relatively short timescales and must be repeatedly re-excited via a swing-amplifier, while Sellwood & Kahn (1991) presented the interesting alternative “groove mode” mechanism for their initial excitation, in which spiral structure is produced by a pinching of the disk. Sellwood (2000) has also argued that almost all numerical simulations strongly support the notion that spiral structure is transient; indeed recent attempts to impose any kind of long-lived spiral density wave on a numerical simulation only seem to work if the spiral structure is very tightly wound up (Yano, Kan-Ya & Gouda 2003), which is not what one finds in many real grand-design

spirals. From an observational perspective, it has also often been noted that the most dramatic spiral galaxies like M51 all seem to have interacting companions, which suggests that such interactions play a role in continuously exciting an evolving spiral structure. This anecdotal impression was borne out in the study by Elmegreen & Elmegreen (1983), which showed that grand design spirals are significantly more common in group environments where such interactions will be more frequent.

There therefore remains the most basic question about the spiral structure that defines the appearance of so many galaxies: how long does it persist, or, put more evocatively, how long could extragalactic travellers stay away and still recognize their own galaxy when they got home? This question is of more than purely navigational interest, as the longevity of spiral structure has fundamental implications for our understanding of galaxy formation and evolution. The interpretation of the Hubble sequence depends strongly on the duty cycle of the open, grand design spiral structure that defines the late end of the sequence, while the timescales for dynamical evolutionary processes such as the heating of the stellar component by spiral arms (Jenkins & Binney 1990) also clearly depend on how long these structures last.

The degree to which a pattern persists is dictated primarily by whether it has a single “pattern speed,” Ω_p , the angular rate at which the pattern rotates. One of the difficulties in studying this quantity is that it has no simple relation to the more directly observable physical velocity of material at different radii in the galaxy. The situation is

* E-mail: michael.merrifield@nottingham.ac.uk

further complicated by the fact that only one component of this velocity is directly accessible through the Doppler shift. However, Tremaine & Weinberg (1984, hereafter TW) elegantly demonstrated that one can invoke the continuity equation to derive Ω_p from the observable material kinematics solely by making the assumptions that the kinematic tracer is conserved, that it orbits in a single plane, and that the pattern rotates rigidly, so that Ω_p is a single well-defined constant. Specifically, one can write the continuity equation as

$$\frac{\partial}{\partial t}\Sigma + \frac{\partial}{\partial x}\Sigma v_x + \frac{\partial}{\partial y}\Sigma v_y = 0, \quad (1)$$

where $\Sigma(x, y, t)$ is the surface density of material orbiting in a plane with the Cartesian coordinates chosen to be aligned with the galaxy's observed major and minor axes. TW showed how one can integrate this equation twice to get rid of the unobservable velocity component and eliminate the numerically-unstable spatial derivatives, leaving

$$\Omega_p \int_{-\infty}^{\infty} \Sigma x dx = \int_{-\infty}^{\infty} \Sigma v_y dx. \quad (2)$$

The terms in both integrals are all measurable (v_y is just the observable line-of-sight velocity corrected for the galaxy's inclination). These integrals can be determined for a range of cuts at different distances y from the galaxy's major axis. In principle, each such cut provides an independent measurement of Ω_p , but a more robust approach to calculating the pattern speed involves making a plot of one of these integrals suitable normalized, $\langle x \rangle = \int \Sigma x dx / \int \Sigma dx$ against the other with the same normalization, $\langle v_y \rangle = \int \Sigma v_y dx / \int \Sigma dx$: such a plot should yield a straight line passing through the origin, whose slope is Ω_p (Merrifield & Kuijken 1995).

The TW technique has now been successfully applied to a number of barred galaxies, using stars as the tracer population and optical absorption line spectroscopy to measure their kinematics, with the interesting result that these objects do have well-defined pattern speeds and are rapidly rotating (Aguerri, Debattista & Corsini 2003; Gerssen, Kuijken & Merrifield 2003; Corsini 2004). However, analyses of spiral galaxies have generally proved less straightforward for several reasons. First, spiral structure is geometrically a good deal more complicated than a bar. This more complex structure means that some parts of the structure may be at an orientation in which the TW method has no discriminatory power (essentially because $\langle x \rangle$ and $\langle v_y \rangle$ both become very small). It is also the case that some parts of the complex spiral structure are clearly transient features that take no part in any global pattern rotation, but can nonetheless produce significant spurious signal in the TW analysis. Fortunately, the fact that we can choose the values of y to which the analysis is to be applied means that we can to a large extent avoid the regions compromised in this way. A second issue is that obscuration and star formation in spiral arms mean that application of the continuity equation to the observable stellar component of these systems may not be valid (although may perhaps be possible using near infrared emission). The technique has therefore usually been applied to radio observations of the gaseous components, either in HI (e.g. Westpfahl 1998) or CO (e.g. Rand & Wallin 2004), to avoid problems of obscuration. Formally, conversion of gas into stars means that the continuity equation

is not applicable to this tracer, either, but star formation does not have the disproportionate effect on gas that bright young stars have on the optical emission, so the analysis is not unduly compromised.

The most interesting problem in the application of the TW method to spiral galaxies, however, is that even after the above issues have been dealt with the method still seems to break down because plots of $\langle x \rangle$ against $\langle v_y \rangle$ do not yield straight lines for any choice of major axis position angle [Debattista (2003) and Rand & Wallin (2004) explore in detail how such plots can be sensitive to this parameter]. In some cases, the departures from a line can be attributed to the limited quality of the data, but in others clear systematic departures from the linear fit are apparent. By far the simplest interpretation of this failure is that these spiral arms do not have a single pattern speed, so their structure must indeed be evolving with time.

In principle, one can use this breakdown of the TW method to constrain the spatial variation in Ω_p and hence the lifetime of the current spiral structure. However, the original TW method was not particularly well formulated for such an analysis because the integrals in equation (2) combine data from a wide range of radii, so they produce complicated spatially-averaged estimates of any varying pattern speed, which have no simple physical interpretation. Westpfahl (1998) was able to use these values to derive the spatial variation in Ω_p under the assumption that it only changes slowly with position, but such slow variations are by no means guaranteed. He also presented a generalization of the technique that resulted in a tractable integral equation if Ω_p only varies with position along the major axis of the galaxy, x , but since this choice of Cartesian coordinate arises simply from the viewing angle and not any intrinsic property of the galaxy, the pattern speed will not in reality depend solely on this coordinate.

This paper therefore revisits the problem and derives a generalization of the TW method in which the pattern speed is allowed to vary arbitrarily rapidly in the radial direction within the galaxy. This is not the only possible way that Ω_p could vary spatially, but it is the simplest physically-motivated option. It explicitly allows for the possibility that a galaxy may contain a number of distinct features at different radii, such as bars and spiral arms, each with their own pattern speeds, and it also permits one to calculate a simple metric of the lifetime of a galaxy's current pattern. The remainder of this paper is laid out as follows. Section 2 presents the mathematical generalization of the TW method to a pattern speed that varies with radius, and Section 3 gives an example of its application to the grand design spiral galaxy NGC 1068. Finally, conclusions are drawn in Section 4.

2 THE GENERALIZED TW METHOD

Even if the pattern speed is allowed to vary with radius within a galaxy, it is still the case that the pattern at a given radius simply rotates around in azimuth ϕ with time, so one can replace the temporal derivative in equation (1) with

$$\frac{\partial \Sigma}{\partial t} = -\Omega_p(r) \frac{\partial \Sigma}{\partial \phi}, \quad (3)$$

as in the original TW analysis. Making this substitution in equation (1), and integrating over all values of x to eliminate the unobservable v_x component of velocity, we find

$$\int_{-\infty}^{\infty} \Omega_p(r) \frac{\partial \Sigma}{\partial \phi} dx - \int_{-\infty}^{\infty} \frac{\partial}{\partial y} \Sigma v_y dx = 0. \quad (4)$$

Still following TW, we now integrate over y to eliminate a noise-sensitive spatial derivative, yielding

$$\int_{y'=y}^{\infty} \int_{x=-\infty}^{\infty} \Omega_p(r) \frac{\partial \Sigma}{\partial \phi} dx dy' + \int_{-\infty}^{\infty} \Sigma v_y dx = 0. \quad (5)$$

Changing variables from Cartesians to polars in the double integral gives

$$\int_{r=y}^{\infty} \int_{\phi=\arcsin(y/r)}^{\pi-\arcsin(y/r)} \Omega_p(r) \frac{\partial \Sigma}{\partial \phi} r dr d\phi + \int_{-\infty}^{\infty} \Sigma v_y dx = 0, \quad (6)$$

and carrying out the integration with respect to ϕ then yields the final integral equation,

$$\int_{r=y}^{\infty} \{ [\Sigma(x', y) - \Sigma(-x', y)] r \} \Omega_p(r) dr = \int_{-\infty}^{\infty} \Sigma v_y dx, \quad (7)$$

where $x'(r, y) = \sqrt{r^2 - y^2}$. As a check, it is straightforward to show that equation (7) reduces to equation (2) in the case where Ω_p is constant.

These coordinates can be straightforwardly constructed from the observed coordinates, allowing for the galaxy's inclination: $x = x_{\text{obs}}$, $y = y_{\text{obs}} / \cos i$ and $v_y = v_{\text{obs}} / \sin i$. Since the kernel term in curly brackets and the integral on the right hand side of equation (7) are both observationally-determined quantities, the problem is now reduced to a Volterra integral equation of the first kind for $\Omega_p(r)$. Such equations are straightforward to solve numerically (Press et al. 1992, chapter 18): reduction of the integral to a discrete quadrature for different values of $r = r_i$ and $y = y_j$ turns this problem into a matrix equation of the form

$$\sum_{r_i > y_j} K(r_i, y_j) \Omega_p(r_i) = f(y_j). \quad (8)$$

The infinite upper limit on the integral complicates the analysis a little, but as for the original TW method one finds that the decline in Σ with radius and the lack of strong spiral structure at large radii mean that the kernel decreases rapidly to zero, so that the integral has converged at an attainable radius. The lower limit on the integral means that the matrix \mathbf{K} is triangular, and hence that equation (8) is readily soluble by back substitution to obtain $\Omega_p(r_i)$. However, the triangular form of the matrix does mean that a problem with the data at some radius will propagate inward to compromise all the derived pattern speeds at smaller radii, so a degree of care must be taken in evaluating the range of radii over which pattern speeds can be determined reliably. Note, though, that in principle one gets two independent measurements of $\Omega_p(r)$, doubling the chances of finding a region free of such issues: here we have assumed that $y > 0$, but we could equally well derive the function from the data at $y < 0$.

As formulated here, Ω_p can vary arbitrarily with radius. One could impose a degree of smoothness by regularizing the solution through an algorithm that penalizes rapid fluctuations in $\Omega_p(r)$, or even by finding a suitably-parameterized

smooth function that best matches the two sides of equation (7). However, for this initial test we will avoid imposing any such prejudice upon the answer, as there is always a danger that a regularized solution owes its form more to the prior assumption about the smoothness of the function than the unpredictable astronomical truth. This freedom is particularly valuable in studies of pattern speed, where spatially distinct features can have completely different pattern speeds, leading to possible discontinuities in $\Omega_p(r)$.

Once the variation in pattern speed with radius has been calculated from the solution of equation (8), it is simple to evaluate how the current spiral pattern will evolve into the future. By following this shearing, different metrics of the lifetime of the spiral structure can be constructed. One straightforward model-independent measure is provided by calculating the dispersion in the derived values of $\Omega_p(r_i)$, $\sigma(\Omega_p)$; a measure of the lifetime of the pattern is then just $2\pi/\sigma(\Omega_p)$. Even simpler, one can just take the largest and smallest values within some range of radii, and calculate a characteristic wind-up time for this part of the pattern of $\tau_{\text{wind}} = 2\pi/(\Omega_p^{\text{max}} - \Omega_p^{\text{min}})$.

3 APPLICATION TO NGC 1068

As an initial experiment, we have applied this algorithm to the BIMA Survey of Nearby Galaxies (BIMA SONG; Helfer et al. 2003) CO observations of the grand-design Sb galaxy NGC 1068, which offers a test case well suited to this analysis. Although optically classified as a normal spiral (Sandage & Tammann 1987), albeit one with a Seyfert nucleus, the 2MASS near-infrared observations (Jarrett et al. 2003) reveal a clear central bar, which provides a strong candidate for the driver of the grand design spiral seen in the CO emission. Rand & Wallin (2004) showed that NGC 1068's gas content is dominated by molecular material and that there is not much current star formation, so little of the molecular phase is being converted to or from other phases and the application of the continuity equation to this component alone is valid.

A further concern in the application of the continuity equation to these data is how well the observed CO emission traces the molecular gas surface density, and hence whether the equation can be applied directly to the data. In particular, even within the Milky Way it is known that the conversion between CO emission and molecular gas column, conventionally termed X , shows a metallicity dependence (Brand & Wouterloot 1995), while there is also evidence that X varies linearly with metallicity from galaxy to galaxy (Boselli, Lequeux & Gavazzi 2002). However, as can be seen from Pilyugin, Vílchez & Contini (2004), there is essentially no metallicity gradient in NGC 1068 over the range of radii probed by the data analyzed here, so X should be close to constant. There is also the possibility that X could vary with other parameters. For example, enhanced macroscopic opacity effects, more intense radiation fields, or stronger deposition of CO on to dust grains could render the values of X in spiral arms systematically different from those in lower density regions. However, recent studies of molecular cloud populations in nearby galaxies with higher resolution and sensitivity than previously achieved are not finding any evidence for significant variations in

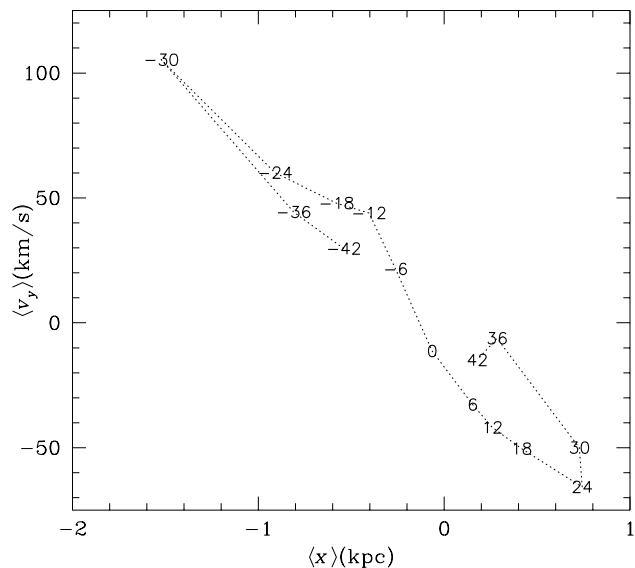


Figure 1. Plot of $\langle x \rangle$ versus $\langle v_y \rangle$ for the BIMA SONG CO observations of NGC 1068. The numbers indicate the distance y_{obs} in arcseconds by which each cut is offset from the galaxy’s major axis, and the dotted line joins adjacent cuts.

X with environment (Rosolowsky et al. 2003; Bolatto et al. 2003; Leroy et al. 2005). Physically, one might expect X to vary with temperature and density as $X \propto T\rho^{-0.5}$ (Young & Scoville 1991); the fact that there is so little observed variation then implies that in the astrophysical environment this combination of temperature and density varies very little in regions where there is a significant amount of molecular material. Interestingly, even if one does allow X to vary by a fairly generous factor of two between the arm and interarm regions, it makes very little difference to a TW-style analysis (Zimmer, Rand & McGraw 2004). Clearly, the matter has not yet been finally settled, and any conclusions will have to carry this caveat, but currently there is no reason to believe that variations in X should compromise this analysis.

What makes NGC 1068 such an interesting target for this analysis is that the conventional TW analysis produced an interesting result for this galaxy (Rand & Wallin 2004). As Figure 1 reiterates, although the plot of $\langle x \rangle$ versus $\langle v_y \rangle$ roughly describes a straight line, it is apparent that there are significant departures from the expected relation. It is also clear that these departures are not the random noise that one would expect if they simply represented a limited signal-to-noise ratio – ordering the points by their distance y_{obs} from the galaxy’s major axis produces a systematic figure-of-eight in this plane. The deviant point at $y_{\text{obs}} = -30$ arcsec arises due to a bright spot in the CO emission that this cut intersects, which is clearly not a part of the overall spiral structure, so, as discussed above, must be avoided in the TW analysis. With the exception of this point, however, NGC 1068 seems to show evidence for a systematic variation in pattern speed with position, warranting further investigation through the analysis developed in this paper.

A preliminary indication of the variation in pattern

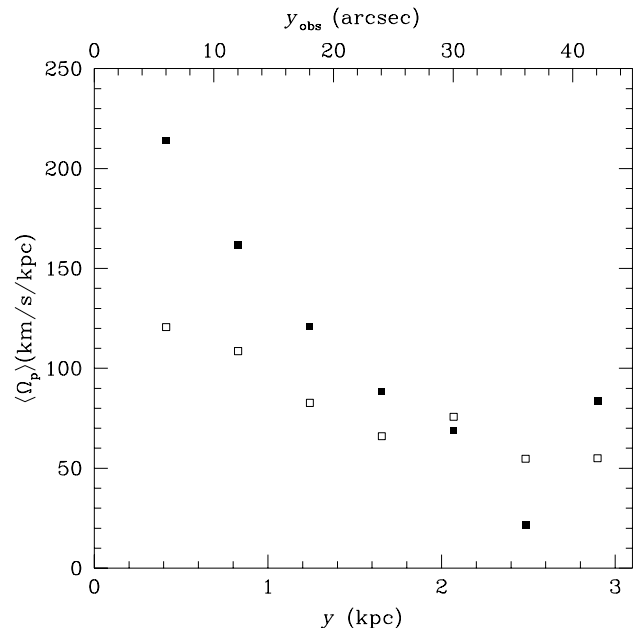


Figure 2. Plot of the weighted mean pattern speed as a function of distance from NGC 1068’s major axis. Filled symbols are for positive y and open symbols show the corresponding values for negative y . The scale conversion from arcseconds to kiloparsecs has been made by adopting a distance to NGC 1068 of 14.4 Mpc (Bland-Hawthorn et al. 1997).

speed with radius can be obtained by calculating $\langle \Omega_p \rangle = \langle v_y \rangle / \langle x \rangle$ for cuts at different values of y_{obs} . Figure 2 shows this quantity for both positive and negative values of y_{obs} . Both sides of the galaxy show a significant decline in $\langle \Omega_p \rangle$ with radius, which, as discussed above, implies that NGC 1068 cannot have a constant pattern speed. In fact, since the value of $\langle \Omega_p \rangle$ at any given value of y_{obs} is a weighted average of the pattern speed at all radii $r \geq y$, this plot will if anything tend to wash out the variation with radius, so we might expect the physical $\Omega_p(r)$ to be an even more steeply declining function. It is also notable that the two sides of the galaxy show a systematic difference in $\langle \Omega_p \rangle$, which provides further evidence that the galaxy cannot be described by a global pattern speed – interestingly, Westpfahl (1998) found a similar difference in his analysis of the spiral structure in M81, suggesting that this phenomenon may be quite common. It should also be noted that the deviant point at $y_{\text{obs}} = -30$ arcsec does not show up dramatically in this plot, as both $\langle x \rangle$ and $\langle v_y \rangle$ are discrepantly large, so their ratio comes out more-or-less in line with the other values. It is only by using the extra information in Figure 1 that the departure from the grand design structure becomes apparent.

Bearing these points in mind, it is still worth seeking to apply the generalized TW analysis to see how rapidly the pattern speed would have to vary with radius to be consistent with the observations. The fact that the two halves of the galaxy show somewhat different properties indicates that the evolution of the pattern must be somewhat more complex than this radial shearing, but it should nonetheless give a reasonable first approximation, and an estimate of the timescale involved for the pattern to evolve significantly.

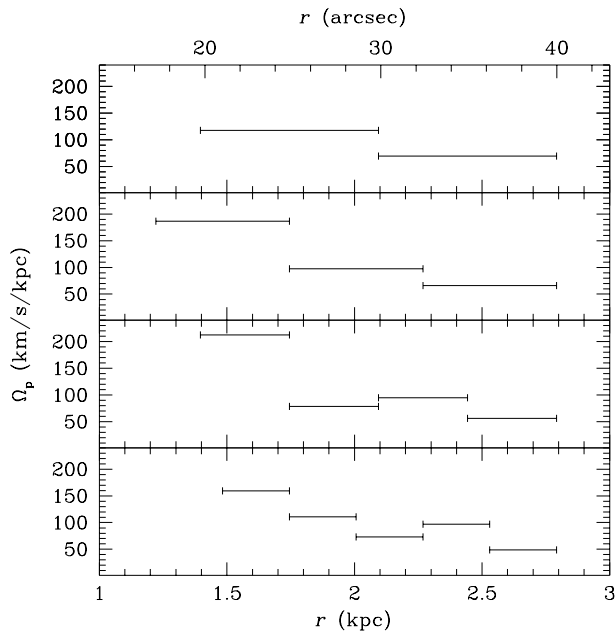


Figure 3. Plot of the variation in pattern speed with radius for NGC 1068, as derived using the generalized Tremaine–Weinberg method. The panels show the results obtained using increasingly finely-binned discretizations of the integral equation (7) to form equation (8).

To this end, we have solved the matrix equation (8) for the data at $y > 0$ (thus avoiding the discrepant point at negative y) to estimate $\Omega_p(r)$. To test the robustness of the result and estimate the associated errors, Figure 3 shows this analysis repeated using different radial binnings to discretize the integral equation (7) into the matrix equation (8). Even for these “well-behaved” data, the matrix inversion method fails inside ~ 20 arcsec. At these radii, the galaxy becomes close to axisymmetric, making the integrals in equation (7) small and meaning that noise starts to dominate. The further amplification of this noise by the inversion process then leads to wildly oscillating random values of Ω_p , a clear sign of numerical instability. However, at larger radii the different binnings produce very consistent rather smooth answers, indicating that the solution to equation (7) is numerically stable in this region even without regularization. The variations between different binnings give a good indication of the uncertainty in $\Omega_p(r)$: although there are variations between the different binnings, the overall decline in Ω_p with radius is robustly reproduced. As Figure 2 already suggested, the pattern speed decreases strongly from ~ 150 km/s/kpc at $r \sim 1.5$ kpc to ~ 50 km/s/kpc at $r \sim 2.5$ kpc. This analysis fits surprisingly well with an entirely independent study undertaken by Schinnerer et al. (2000), who looked at the likely locations for resonances in this galaxy and suggested that if an inner bar existed at $r \sim 14$ arcsec then it should have a pattern speed of ~ 140 km/s/kpc, and that an outer oval-shape distortion which reaches out to $r \sim 120$ arcsec may have a pattern speed as low as ~ 20 km/s/kpc. The advantage of the current study is that we are measuring pattern speeds directly without assuming anything about the resonant radii, such as presuming that the outer oval structure in this system ends at its co-rotation radius. Figure 3

provides direct evidence that the grand-design spiral structure between the inner bar and outer oval is not locked to either of their pattern speeds, but rather that the spiral arm pattern speed varies continuously with radius between these limiting values. This strong shearing implies a short lifetime for the present spiral structure between $r \sim 20$ arcsec and $r \sim 40$ arcsec of only $\tau_{\text{wind}} \sim 10^8$ years, which is directly comparable to (but actually a little shorter than) the corresponding orbital period at these radii. This beautiful grand design spiral would appear to be only a transient feature on the face of NGC 1068.

4 CONCLUSIONS

This paper presents a generalization of the Tremaine–Weinberg method for calculating pattern speeds of galaxies which accommodates the possibility that the pattern speed may vary with radius. This generalization has potential applications to a variety of different galactic systems. One could, for example, attempt to determine the distinct pattern speeds of multiple features within a single galaxy, such as nested bars-within-bars (Corsini, Debattista & Aguerri 2003).

Here, however, we have investigated the apparently simpler case of the grand design spiral structure in the CO emission from NGC 1068. The conclusion of this analysis is that this spiral structure does not have anything close to a single pattern speed, and is winding up on a timescale marginally shorter than the orbital period, reintroducing the winding dilemma with a vengeance. In fact, we know that some of the other assumptions made in the analysis are violated at some level: the difference between the kinematic signal at positive and negative values of y implies that the pattern cannot be evolving with time in a manner entirely consistent with the simplest azimuthal winding up considered here. However, this extra complexity simply means that the current design must be distorting even more profoundly and rapidly than we have found. In the only other comparable study to date, Westpfahl (1998) tentatively reached a similar conclusion regarding the grand design spiral structure in M81, based on both differences between the kinematics of the two sides of the galaxy and the inconsistency of the results from a TW-style analysis. If this result turns out to apply commonly to other galaxies, then intergalactic travellers would be well advised not to use the morphology of spiral structure to identify their homes.

ACKNOWLEDGEMENT

We are very grateful to the referee for helpful comments, which have significantly improved the presentation of this paper. MRM is supported by a PPARC Senior Fellowship, for which he is also most grateful.

REFERENCES

- Aguerri, J.A.L., Debattista, V.P. & Corsini, E.M., 2003, MNRAS, 338, 465

- Bland-Hawthorn, J., Gallimore, J.F., Tacconi, L.J., Brinks, E., Baum, S.A., Antonucci, R.R.J. & Cecil, G.N., 1997, *Ap&SS*, 248, 9
- Bolatto, A.D., Leroy, A., Israel, F.P. & Jackson, J.M., 2003, *ApJ*, 595, 167
- Boselli, A., Lequeux, J. & Gavazzi, G., 2002, *AP&SS*, 281, 127
- Brand, J. & Wouterloot, J.G.A., 1995, *A&A*, 303, 851
- Corsini, E.M., Debattista, V.P. & Aguerri, J.A.L., 2003, *ApJ*, 599, L29
- Corsini, E.M., 2004, in Dettmar, R., Klein, U., Salucci, P., eds, *Baryons in Dark Matter Halos*, SISSA, Trieste, p. 49
- Debattista, V.P., 2003, *MNRAS*, 342, 1194
- Elmegreen, B.G. & Elmegreen, D.M., 1983, *ApJ*, 267, 31
- Gerssen, J., Kuijken, K. & Merrifield, M.R., 2003, *MNRAS*, 345, 261
- Helfer, T.T., Thornley, M.D., Regan, M.W., Wong, T., Sheth, K., Vogel, S.N., Blitz, L. & Bock, D.C.-J., 2003, *ApJS*, 145, 259
- Jarrett, T.H., Chester, T., Cutri, R., Schneider, S.E. & Huchra, J.P., 2003, *AJ*, 125, 525
- Jenkins, A. & Binney, J., 1990, *MNRAS*, 245, 305
- Leroy, A., Bolatto, A.D., Simon, J.D. & Blitz, L., 2005, *ApJ*, 625, 763
- Lin, C.C. & Shu, F.H., 1966, *Proc. Nat. Acad. Sci.*, 55, 229
- Lindblad, B., 1951, *Publ. Obs. Univ. Mich.*, 10, 59
- Merrifield, M.R. & Kuijken, K., 1995, *MNRAS*, 274, 933
- Oort, J.H., 1962, *Interstellar Matter in Galaxies*, p. 234, ed. L. Woltjer, W.A. Benjamin Inc., New York
- Pilyugin, L.S., Vílchez, J.M. & Contini, T., 2004, *A&A*, 425, 849
- Rosolowsky, E., Engargiola, G., Plambeck, R. & Blitz, L., 2003, *ApJ*, 599, 258
- Press, W.H., Teukolsky, S.A., Vetterling, W.V. & Flannery, B.P., 1992, *Numerical Recipes in FORTRAN: The Art of Scientific Computing*. Cambridge University Press, Cambridge
- Rand, R.J. & Wallin, J.F., 2004, *ApJ*, 614, 142
- Sandage, A & Tammann, G.A., 1987, *A Revised Shapley-Ames Catalog of Bright Galaxies*. Carnegie Institute of Washington, Washington D.C.
- Schinnerer, E., Eckart, A., Tacconi, L.J., Genzel, R. & Downes, D., 2000, *ApJ*, 533, 850
- Sellwood, J.A. & Kahn, F.D., 1991, *MNRAS*, 250, 278
- Sellwood, J.A., 2000, *Ap&SS*, 272, 31
- Toomre, A., 1969, *ApJ*, 158, 899
- Tremaine, S. & Weinberg, M.D., 1984, *ApJ*, 282, L5
- Westpfahl, D.J., 1998, *ApJS*, 115, 203
- Yano, T., Kan-Ya, Y. & Gouda, N., 2003, *PASJ*, 55, 409
- Young, J.S. & Scoville, N.Z., 1991, *ARAA*, 29, 581
- Zimmer, P., Rand, R.J. & McGraw, J.T., 2004, *ApJ*, 607, 285